

Preparation and Characterization of ZnS-TiO₂ Nanocomposite

Than Than Win¹, Khin Lay Wai² and Yin Maung Maung³

Abstract

Zinc sulfite (ZnS) and titanium dioxide (TiO₂) nanocomposite were produced using commercially available ZnS and TiO₂ powder. The mechanical milling was used to prepare ZnS-TiO₂ powder in a ball-mill up to 5 h. ZnS-TiO₂ composite was formed by solid state reaction at 500 °C. X-ray diffraction (XRD) technique, scanning electron microscopy (SEM) and UV-vis spectroscopy were utilized to study the structure and optical properties of the nanocomposite powders. The size of particle in the sample was estimated by the Scherrer method. XRD pattern showed that ZnS particles exhibited cubic structure with 5.44 nm average crystallite size. The TiO₂ particles had tetragonal structure with 63.72 nm average crystallite size. X-ray diffraction (XRD) investigation was also performed to examine the structural properties of ZnS-TiO₂ composite. The microstructure, morphology, and texture of the materials system were analyzed by SEM. The results from SEM showed the porous structure. The optical absorption method was successfully used to determine the refractive index (n), absorption coefficient (α) and optical band gap (E_g) of nanocomposite in the wavelength range 200-1000 nm. The experimental data resulted from this research, ZnS-TiO₂ nanocomposite is quite suitable, credible and applicable in use for photovoltaic device.

Keywords: Nanocomposite, X-ray diffraction, Scanning electron microscopy, UV-vis spectroscopy

-
1. Associate Professor, Physics Department , Mandalay University of Distance Education
 2. Lecturer, Department of Engineering Physics, West Yangon Technological University
 3. Associate Professor, Physics Department, Mandalay University

I. Introduction

TiO₂ is considerable interest for both scientific and technical applications. Titanium dioxide or titania (TiO₂) was first produced commercially in 1923. It is obtained from a variety of ores [Dhair T.A.AL]. The bulk material of TiO₂ is widely nominated for three main phases of Anatase , Rutile, and Brookite . Among them, the TiO₂ exists mostly as Rutile and Anatase phases which both of them have the tetragonal structures. However, Rutile is a high-temperature stable phase and Anatase is formed at a lower temperature [Lalitha G]. Titania is used in medical applications, cosmetics, catalysts, photocatalysts, gas sensors, lithium batteries, biomolecular sensors and dye-sensitized solar cells. TiO₂ as photocatalyst have been widely used in the degradation of organic dyes due to stability of their chemical structure, non-toxicity, optical and electrical properties. In order to enhance the efficiency of photocatalysts, it is necessary to search for, and study, new catalysts [Yoshitake M].

ZnS is II-VI compound semiconductor with direct and wide band gap of 3.68 eV at room temperature and widely used as a phosphor in optical devices. ZnS has been used as optical devices, such as ultraviolet light emitting diodes, flat panel display, solar cells, and optical sensors. ZnS particles have two kinds of structures, zinc blende structure (cubic crystal) and wurtzite structure (hexagonal). The cubic phase is the stable low temperature and at room temperature while the dense hexagonal structure is stable above 1020°C at atmospheric pressure [Parvaneh I][Arup K.K et al]. ZnS nanocrystals started converting into the WZ phase at 400°C temperature and the formation of the high-temperature WZ phase of ZnS was found after annealing at 400-525°C temperature in vacuum [Ruby C] [Damian C.O]. ZnS is one of the most applied semiconductors in optical devices due to its high refracted index and high transmission within the visible range [Dhatshanamurthi P][Michael F.R]. The photoelectrical properties make ZnS particles as a very promising material in solar cell application [Khalid T.Al-R]. The interaction between the ZnS and TiO₂ phases, and the strong adsorption to the substrate at the ZnS/TiO₂ composite surface, are responsible for this enhanced photocatalytic activity [Tiwary K.P] [Fitria R]. The synthesis of ZnS coupled with semiconductor TiO₂, which induces the optical

response towards visible region [LaxmiV.N.R. et al]. The photocatalytic activity of the ZnS-TiO₂ composite strongly depends not only on the structure of the support but also on the specific interaction between ZnS and support [Ze-Da M].

In the present work the preparation and characterization of ZnS-TiO₂ composite by solid state reaction method was studied.

II. Experimental

2.1. Preparation of ZnS-TiO₂ Composite

Commercial ZnS and TiO₂ powder (Aldrich) were used as starting chemicals. Initially ZnS and TiO₂ were characterized by X-ray diffraction (XRD) for purification. After that ZnS and TiO₂ were mixed with methanol by solid state mixed oxide route by equal molar ratio. Mechanochemical milling process was performed to form the homogeneous and small particle size. Ball milling process was performed for 5 h. After ball milling, ZnS-TiO₂ was annealed at 500°C for 1 h in O₂ ambient. And then it was ground to fine powder by using agate motor for about 9 h. It was sieved by 3-stages mesh (100, 150, 200) and uniform particle sized powder was formed. Figure 1 showed ZnS – TiO₂ composite powder preparation sequence diagram.

2.2. Characterization of ZnS-TiO₂ Composite

X-ray diffraction (XRD) was employed to study the crystal structure and phase analysis of all samples. The diffraction pattern was recorded on RIGAKU MiniFlex 600 diffractometer with Cu-K_α radiation ($\lambda = 1.54060 \text{ \AA}$), over the range of $2\theta = 10^\circ$ to 70° . The crystallite size was calculated using the Scherrer equation. The grain size and morphology of the composite were determined by Scanning Electron Microscope (SEM) by using AURIGA 45-07. Using UV-visible absorption spectrum of composite was recorded on SHIMADZU 1800 spectrophotometer was studied.

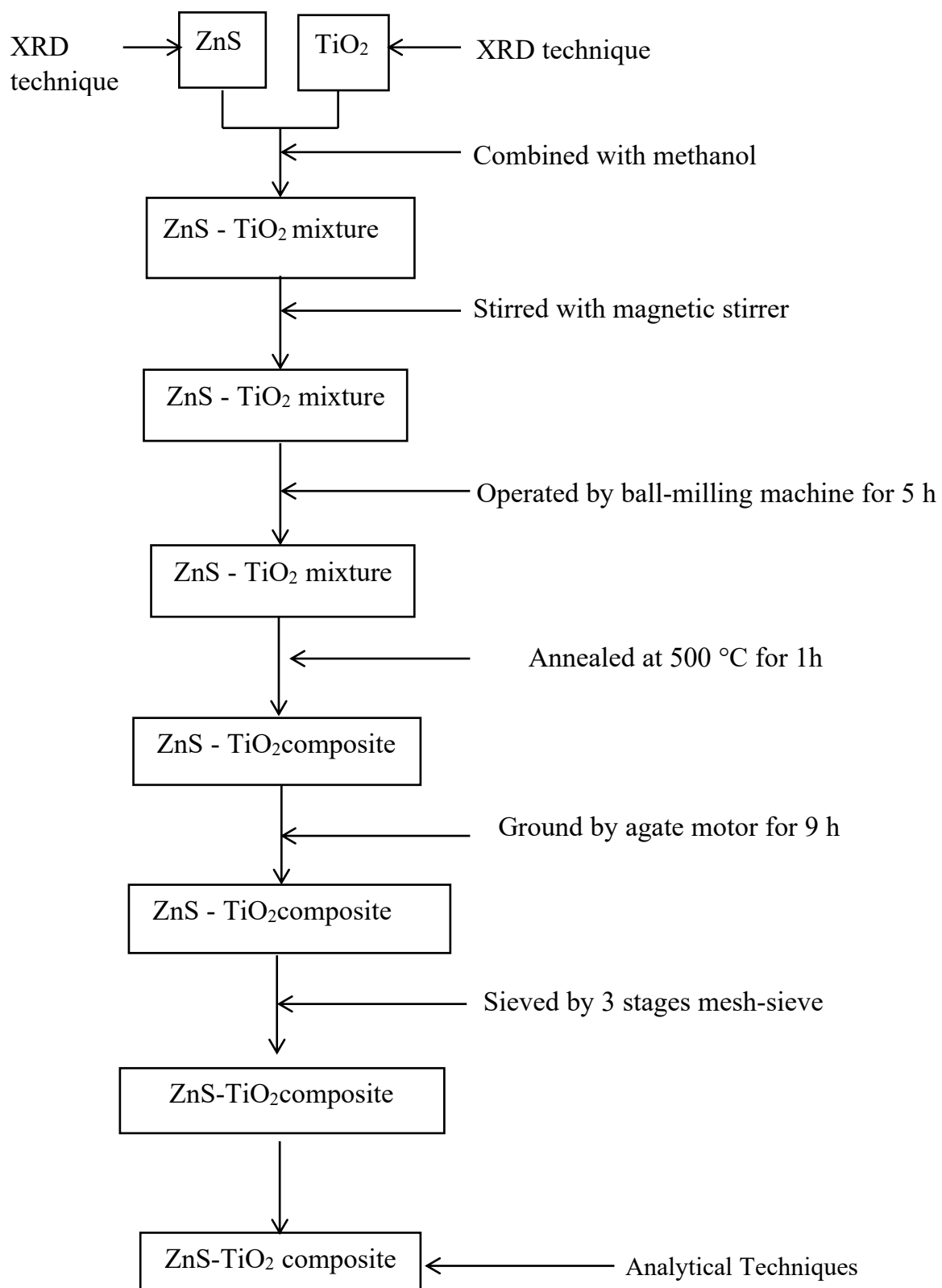


Figure 1 ZnS – TiO₂ composite powder preparation sequence

III. Results and Discussion

3.1 XRD analysis

Figure 2 (a) represented with the XRD pattern for TiO₂ powder. The lattice parameters were observed to be $a = b = 3.766 \text{ \AA}$ and $c = 9.478 \text{ \AA}$ for anatase TiO₂ powder with the tetragonal symmetry. The lattice distortion (c/a) of TiO₂ powder is 2.516. The volume of unit cell was 134.488 \AA^3 . Table 1 showed comparison for diffraction angles of all identified peaks for TiO₂ powder between observed sample and Lalitha G, 2015. Table 2 showed comparison for lattice constants and c/a of all identified peaks for TiO₂ powder between observed sample and Lalitha G, 2015 .

Figure 2 (b) represented the XRD pattern for ZnS powder. The lattice parameters were examined to be 5.370 \AA and unit cell volume was 154.862 \AA^3 for ZnS powder with cubic symmetry. Table 3 showed comparison on diffraction angles of all identified peaks for ZnS powder between observed sample and Khalid T. Al- R, 2014.

The XRD profile of ZnS-TiO₂ composite powder with equal molar ratio was shown in Figure 2(c). In this composite material, the lattice parameters were observed to be $a = b = 3.77 \text{ \AA}$ and $c = 9.49 \text{ \AA}$ for anatase TiO₂ composite with tetragonal symmetry and the volume of unit cell was 134.88 \AA^3 . The lattice parameters were also observed to be $a = b = 3.81 \text{ \AA}$ and $c = 43.63 \text{ \AA}$ for ZnS composite with hexagonal symmetry and the volume of unit cell is 548.486 \AA^3 . As the result, ZnS converted from cubic phase to hexagonal phase at 500°C . The crystallite size was determined using the Scherer's equation.

$$D = \frac{K \lambda}{\beta \cos \theta}$$

Where, D is the crystallite size, λ is the wavelength of X-rays (1.54056 \AA), β is the full width at half maximum of the diffraction peak, and θ is the Bragg diffraction angle. The FWHM and crystallite size of TiO₂ powder, ZnS powder and ZnS-TiO₂ composite powder are described in Table.4, 5, 6 and 7.

Table 1 Comparison on the diffraction angles of all identified peaks for TiO₂ powder between observed sample and Lalitha G, 2015

No	Dominate Peak	Diffraction angle, 2 theta (deg)	
		Observed	Lalitha G. et al ,2015 Journal of Saudi Chemical Society
1	(1 0 1)	25.54	25.3
2	(1 1 2)	38.78	38.1
3	(2 0 0)	48.25	47.4
4	(1 0 5)	54.09	54.3
5	(2 1 3)	62.30	62.1

Table 2 Comparison on lattice constants and c/a of all identified peaks for TiO₂ powder between observed sample and Lalitha G,2015

No	TiO ₂ powder	Lattice parameter (Å)		c/a
		a	c	
1	Observed	3.766	9.478	2.516
2	Lalitha G. et al, 2015 Journal of Saudi Chemical Society	3.826	9.403	2.457

. Table 3 Comparison on the diffraction angles of all identified peaks for ZnS powder between observed sample and Khalid T. Al- R, 2014

No	Dominate Peak	Diffraction angles 2theta (deg)	
		Observed	Khalid T. Al- R, 2014
1	(1 1 1)	28.771	28.715
2	(2 2 0)	47.872	48.466
3	(3 1 1)	56.815	57.500

Table 4 FWHM and crystallite size of TiO₂ powder for all identified peaks

No	Peak	FWHM (deg)	Crystallite size (nm)
1	(1 0 1)	0.155	52.40
2	(1 0 3)	0.130	64.39
3	(0 0 4)	0.144	58.27
4	(1 1 2)	0.129	65.20
5	(2 0 0)	0.126	68.83
6	(1 0 5)	0.140	63.63
7	(2 1 1)	0.131	68.00
8	(2 1 3)	0.134	69.19
9	(2 0 4)	0.140	66.42
10	(1 1 6)	0.158	60.91
Average crystallite size			63.72

Table 5 FWHM and crystallite size of ZnS powder for all identified peaks

No.	Peak	FWHM (deg)	Crystallite size (nm)
1	(111)	1.59	5.14
2	(220)	1.82	4.77
3	(311)	1.70	5.31
Average crystallite size			5.07

Table 6 FWHM and crystallite size of TiO₂ in ZnS- TiO₂ composite for all identified peaks

No	Peak	FWHM(deg)	Crystallite size(nm)
1	(1 0 1)	0.156	52.10
2	(1 0 3)	0.139	60.20
3	(0 0 4)	0.138	60.79
4	(1 1 2)	0.150	56.06
5	(2 0 0)	0.123	70.48
6	(1 0 5)	0.138	64.52
7	(2 1 1)	0.130	68.86
8	(2 1 3)	0.260	35.63
9	(2 0 4)	0.144	64.55
10	(1 1 6)	0.159	60.50
	Average crystallite size		59.37

Table 7 FWHM and crystallite size of ZnS in ZnS- TiO₂ composite for all Identified peaks

No	Peak	FWHM(deg)	Crystallite size(nm)
1	(0 1 1)	0.272	30.00
2	(1 0 4)	0.210	38.95
3	(0 0 14)	0.285	28.73
4	(1 0 7)	0.220	37.39
5	(0 1 16)	0.670	12.71
6	(1 1 1)	0.280	30.98
7	(1 0 21)	0.260	33.94
8	(0 2 4)	0.304	29.63
	Average crystallite size		30.29

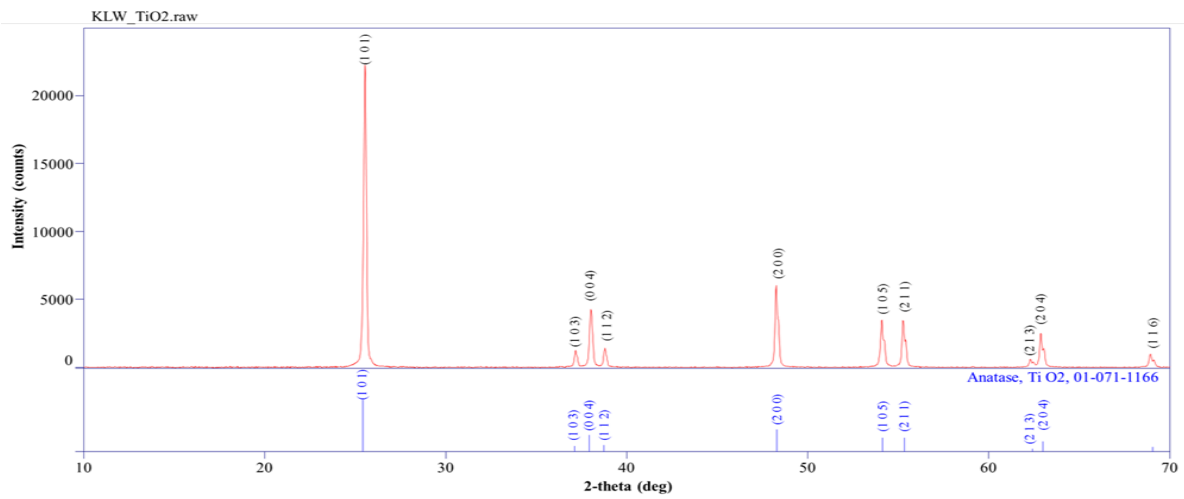


Figure 2(a) XRD pattern of TiO₂ powder

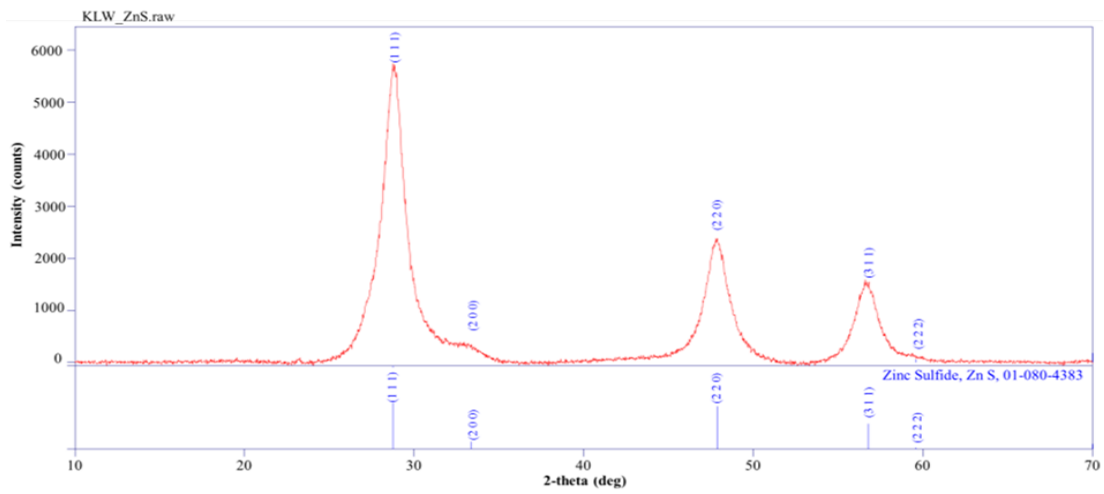


Figure 2(b) XRD pattern of ZnS powder

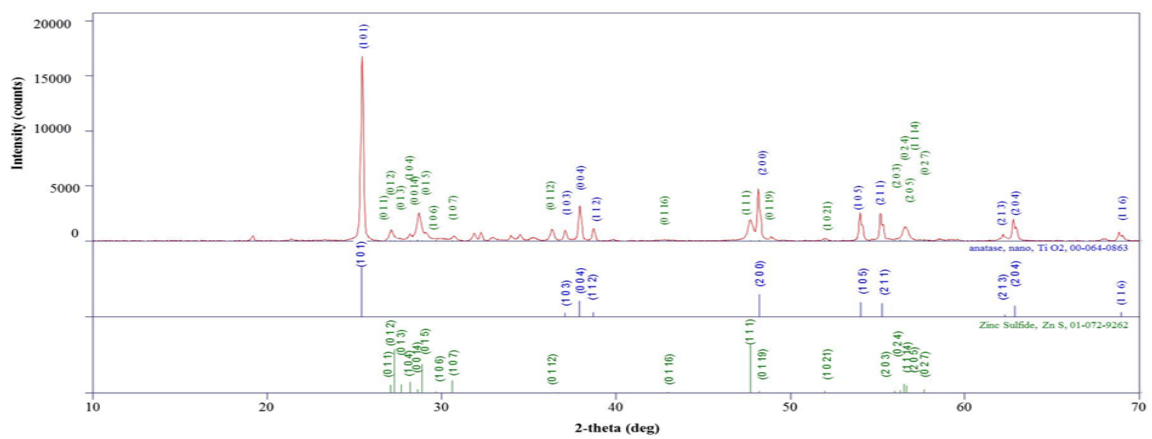


Figure. 2(c) XRD pattern of ZnS-TiO₂ composite

3.2 SEM Analysis

The morphology and grain size of the prepared ZnS-TiO₂ composite were investigated by SEM. Figure 3 showed the morphologies of ZnS-TiO₂ composite. It was observed from micrograph, particle size was found to be about 57.42 nm. The particle size and crystallite size observed in both SEM and XRD measurement were found to be nearly equal.

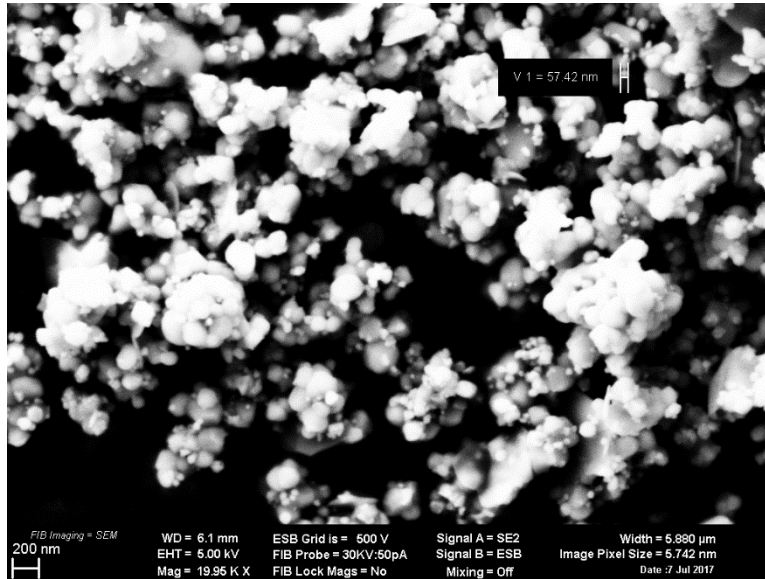


Figure 3 SEM image of ZnS-TiO₂ composite.

3.3 UV-vis Analysis

UV-vis absorption spectroscopy is widely used tool for checking the optical properties of nanosized particles. Figure 4 showed the absorption spectrum of ZnS-TiO₂ composite. The transmission spectrum of ZnO-TiO₂ composites were described in Figure 5. For ZnS-TiO₂ composite, optical transition has been shown to be direct. The variation in the absorption coefficient as a function of photon energy for allowed direct is given by

$$\alpha (h \nu) = A (h \nu - E_g)^{1/2}$$

Where, α is the absorption coefficient, A is a constant, h is Planck's constant, ν is the frequency, and E_g is the band gap energy. Fig 4 showed the UV-vis absorption spectrum of ZnS-TiO₂ composite. From the spectrum three peaks were observed at

197.5 nm, 204 nm and 227.5 nm. The absorbance and relation wavelength of composite was described in Table 8. A plot of $(\alpha hv)^2$ versus photon energy (hv) showed intermediate linear region, the extrapolation of the linear part can be used to calculate the E_g from intersect with hv axis as shown in Figure 6. The resultant value of E_g for ZnS-TiO₂ composite was found to be about 3 eV. Variation of extinction coefficient (k) with wavelength was shown in Figure 7. The small value of extinction coefficient indicated that the composite sample still were transparent to electromagnetic radiation. Figure 8 showed the plot of the refractive index (n) as a function of the wavelength and it could be noticed that the refractive index decreases abruptly as the wavelength increases. The variation in refractive index (n) and extinction coefficient (k) values with the wavelength revealed that some interaction took place between photons and electrons of the composite (Vaishali B).

Table 8 Absorbance and wavelength of ZnS-TiO₂ composite from absorption spectrum

No	Absorbance (a.u)	Wavelength (nm)
1	0.474	227.5
2	2.918	204.0
3	-3.273	197.5

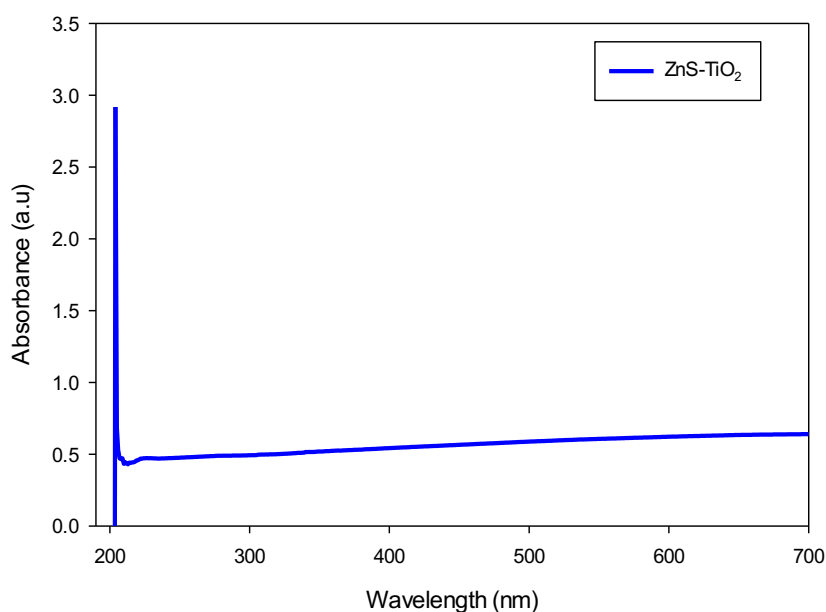


Figure 4 Absorption spectrum of ZnS-TiO₂ composite

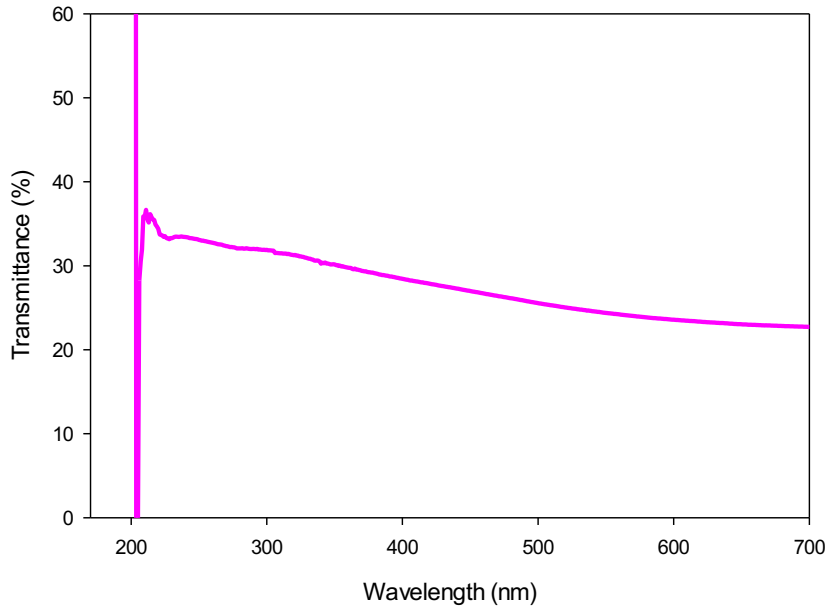


Figure 5 Transmission spectrum of ZnS-TiO₂ composite

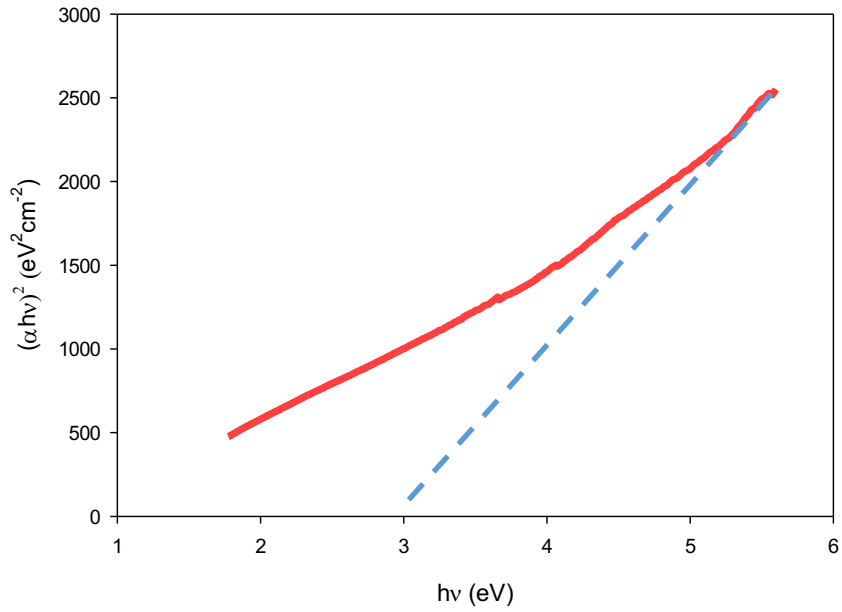


Figure 6 plot of $(\alpha hv)^2$ versus photon energy ($h\nu$) of ZnS-TiO₂ composite

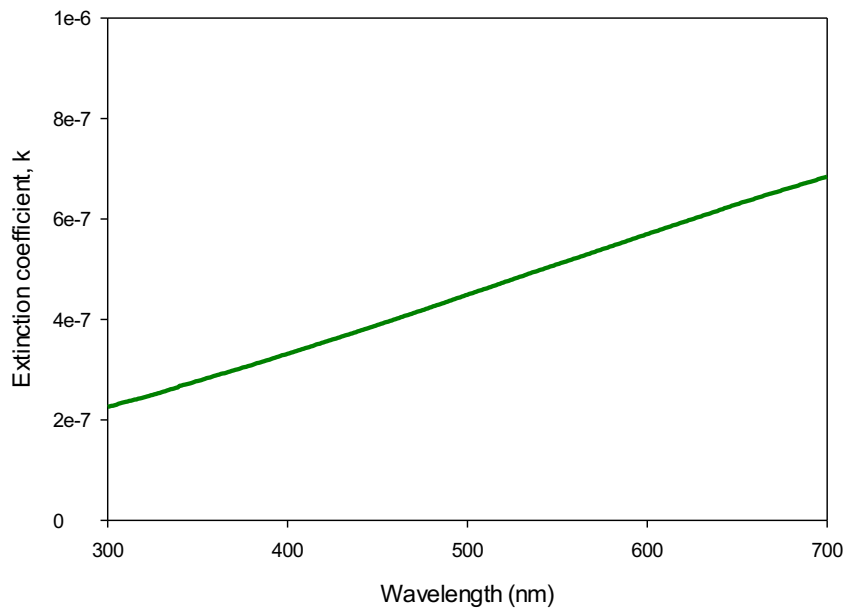


Figure 7 Variation of extinction coefficient with wavelength of ZnS-TiO₂ composite

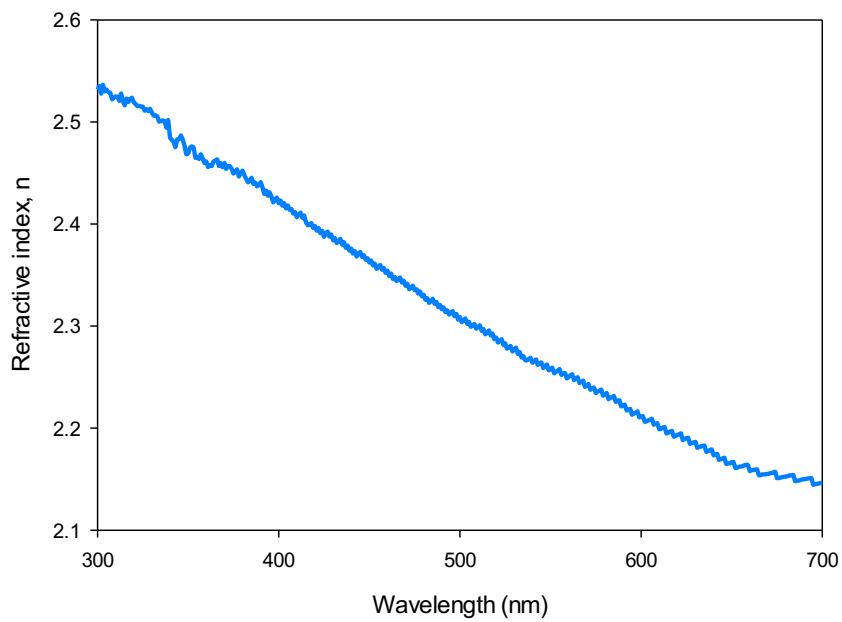


Figure 8 Variation of refractive index with wavelength of ZnS-TiO₂ composite

Conclusion

Preparation and characterization of ZnS-TiO₂ composite had been implemented. The XRD and SEM results give the nanocomposite of ZnS-TiO₂ materials system. The crystallite size of composite obtained XRD result and grain size of composite from SEM are almost the same and leading to single crystal. The efficiency of solar cell may be large because of wide value of band gap energy. The refractive index is small at the large wavelength region and reveals the better performance of solar cell. According to the experimental data resulted from this research, ZnS-TiO₂ nanocomposite is quite potential candidate for use in photoanode of dye-sensitized solar cell (DSSC).

Acknowledgements

We would like to express my profound gratitude to Dr Tin Maung Hla, Rector, Mandalay University of Distance Education who gives us permission to read this paper. We would to acknowledge our deep gratitude to Professor Dr Kathi Nwe, Head of Department of Physics, Mandalay University of Distance Education, for allowing and encouraging us to present this paper. We are also grateful to Professor Dr Khin Khin Win, Head of Department of Physics, University of Yangon, for the supply of preparation equipment and use of XRD apparatus. We are thankful to Department of Research and Innovation for SEM Analysis. We are also thankful to AMTT Company for UV-vis Measurement.

References

- Arup K.K. and Pathik K., "Cubic-to-Hexagonal Phase Transition and Optical Properties of Chemically Synthesized ZnS Nanocrystals" Results in Physics, Vol.2, (2012), P.150
- Damian C.O., "ZnS, CdS and HgS Nanoparticles via Alkyl-Phenyl

Dithiocarbamate Complexes as Single Source Precursors”,
International Journal of Molecular Sciences, Vol.12, (2011), P.5539

Dhatshanamurthi P, “Highly Active ZnS Loaded TiO₂ Photocatalyst for
Mineralization of Phenol Red Sodium Salt under UV-A Light”,
Indian Journal of Chemistry, Vol.53 (A), (2014), P.20

Dhair T.A.AL, “Quantitative Phase Analysis for Titanium Dioxide from X-Ray
Powder Diffraction Data Using The Rietveld Method”, Diyala
Journal For Pure Sciences, Vol.9, Issue No.2, (2013), P.108

Fitria R, “The Optical Properties and Photocatalytic Activity of ZnS-TiO₂/
Graphide Under Ultra Violet and Visible Light Radiation” Bulletin of
Chemical Reaction Engineering and Catalysis, Vol. 10, Issue No. 3,
(2015), P. 294

Khalid T.Al-R, “Synthesis, Structure And Characterization of ZnS, Qds And
Using It Photocatalytic Reaction”, International Journal of Scientific and
Technology Research, Vol. 3, Issue No. 5, (2014), P. 214

Lalitha G, “Synthesis and Characterization of TiO₂ Quantum Dots for
Photocatalytic Application”, Journal of Saudi Chemical Society, Vol.
19, Issue No. 5, (2015), P. 590-591

Laxmi V.N.R. , Shekharam T., Hadasa K., Yellaiah and Nagabhusanam M.,
“Synthesis and Study of Structural, Optical Properties of Co_xZn_{1-x}S
Semiconductor Compounds”, IOSR Journal of Applied Physics, Vol.5,
Issue No. 1, (2013), P. 19

Michael F.R, “Synthesis, Structural, Optical and Dielectric Properties of ZnS
Nanoparticles for the Fabrication of DSSCs”, International Journal of
Scientific Research and Modern Education, (2016)

Parvaneh I, “Characterization of ZnS Nanoparticles Synthesized by
Co-precipitation Method , Chin.Phys,B, Vol. 24, Issue No. 4, (2015), P.
046104-1

- Ruby C, “Characterization of Chemically Synthesized Mn doped ZnS Nanoparticles”, Department of Chemistry SantLongowal Institute of Engg. And Tech. Longowal 148 106 India, Vol. 9, Issue No. 4, (2012)
- Tiwary K.P, “Structural and Optical Properties of ZnS Nanoparticles Synthesized by Microwave Irradiation Method”, Department of Applied Physics Birla Institute of Technology Patna Campus India, Vol. 10, Issue No. 9, (2013)
- Vaishali B, “Study of refractive index dispersion and Optical Conductivity of PPy doped PVC films”, Indian Journal of Pure & Applied Physics, Vol 54, February 2016, pp 105-110
- Yoshitake M, “Synthesis and Phase Transformation of TiO₂ Nano-crystals in Aqueous Solutions”, Journal of the Ceramic Society of Japan, Vol. 117, Issue No. 3, (2009), P.373
- Ze-Da M, “Synthesis and Characterization of ZnS and ZnS/TiO₂ Nanocomposites and Their Enhanced Photo-decolorization of MB and 1, 5-DiphenylCarbazide”, Journal of Korean Ceramic Society, Vol. 51, Issue No. 4, (2014), P. 307